Understanding Space Stations break-ups, a genetic algorithm attempt

S. Sanvido [(1)], S. Lemmens[(2)]

[(1)] LSE Space GmbH at ESA/ESOC Space Debris Office, Darmstadt, Germany, Silvia.Sanvido@esa.int
[(2)] ESA/ESOC Space Debris Office, Darmstadt, Germany, Stijn.Lemmens@esa.int

ABSTRACT

The foreseen nominal end of life of the International Space Station (ISS), pose the natural question if the information collected during previous re-entries of large objects, as for the MIR and the SKYLAB space stations, or cargos vehicle of dimensions similar to space station modules, such as Delta II -Second Stage, could be used to set a baseline to understand and predict the break-up sequence of the ISS or space stations in general.

The proposed work is based on a genetic algorithm approach which makes use of simplified geometries for the re-entry of large objects, in order to provide a statistically significant analysis of the break-up, providing an approximated range of values for some of the quantities which characterize the atmospheric re-entries phenomenology for large objects.

1 INTRODUCTION.

It was the 23rd March 2001 when Hugh Williams of CNN, which for the occasion has travelled until the western shores of Viti Levu, Fiji Islands, pointed his camera on the sky waiting to capture the Russian Space Station MIR during its controlled re-entry. He succeed, shooting 29 seconds, showing some sequential break ups of the MIR space station [1]. A further analysis of the video was able to relate the objects that are visible in the images to the MIR modules and to extract partial information of the break-up sequence [2]. This happened more than 20 years after the re-entry of another Space Station, the United States' SKYLAB [3], which in 1979 underwent a partially controlled re-entry over the Indian Ocean and part of South Western Australia. Some of the Skylab fragments were found in South Western Australia [4], and their on-ground distribution could be used to get insight on its break-up sequence [5].

The MIR and SKYLAB space stations represent the most massive artificial objects to re-enter the Earth atmosphere in one piece, with estimated weight of ~74 and ~120 metric tons respectively. However, these large space stations, as well as the International Space Station (ISS), can be functionally thought of as a combination of their modules, which size and design is more similar to human and cargo vehicle that typically ferry between space station and Earth. As proxy example of this latter class, the uncontrolled re-entry of the DELTA II – Second Stage 2 of total dry mass of 920 kg, occurred on January 22nd 1997 over USA and Canada [7], is here considered as subject of interest, especially because the recovered re-entry debris were some of the most commonly identified, such as propellant and gas tanks.

The major concern which motivates this analyses is the historically high probability of casualties or serious injuries among the human population link to the atmospheric uncontrolled re-entry of space object of mass larger than one ton, which most likely exceeds the various national and international safety standard limits of 1 in 10000 [8]. When the probability of casualty for the uncontrolled re-entry of a space object exceed this threshold, one of the two possible options, alongside the so-called design for demise technology [17] that needs to be implemented during the preliminary design phases, is to perform a controlled re-entry.

The planning of a controlled re-entry, however, is also subject to regulations which require the identification of a target impact area (Safety Re-entry Area, SRA) that can only extend over an ocean unhabituated area, with clearance of landmasses, air and maritime traffic routes and any kind of assets [8]. The risk assessment needs to demonstrate the conformity of the limits of the SRA for a controlled re-entry, for a specific spacecraft, is generally performed using specific tools for the re-entry simulations which employs conservative representation of the physics to trigger the fragmentation, as for example single break-up altitude at 78 km [9].

However, characterizations of break-up physics and of the underlying uncertainties for the re-entry of large structure such as space station is still subject of studies. Preliminary test results under ideal aerodynamic forces suggests a mechanical fragmentation around 75 km for the connection between the ISS as whole and the ESA's Columbus module [10], and that shock impingements prior this mechanical break-up can change the aerothermal behaviour and the demise of the structure as consequence[11].

In order to overcome these limitations and provide insights for the characterization of the break-up scenarios for large re-entering objects, the proposed work utilizes the available heterogeneous information for the aforementioned re-entries, such as altitude and velocity of MIR modules extracted by the CNN video and the footprint of SKYLAB and DELTA II-Second Stage 2, to establishing a methodology based on genetic algorithm

in order to retrieve the most plausible break-up sequence w.r.t. the available observed data. This is done by coupling the observed phenomenology with a simplified physics model, that enables a large number of simulations to be performed and a sequence of possible events to be defined through optimisation, at the expense of accurately predicting the events. Results define a baseline for the break-up phenomenology of large objects, providing a significant insight for the foreseen ISS re-entry.

2 TEST CASES

This work aims to investigate the break-up of large structures such as cargo vehicles and space stations. Therefore, the following three test cases are considered of interest.

2.1 MIR space station

The MIR was a modular space station operating in LEO from 1986 to 2001 and the first space station assembled in orbit from 1986 to 1996.

On the 23rd March 2001, the MIR performed its controlled re-entry over the western part of the Pacific Ocean, under propulsive force provided by the attached Progress spacecraft. [2]. The over-performing final burn of the de-orbiting prevented the possibility to observe the beginning of the atmospheric re-entry from a dedicated airborne observation campaign. However, the re-entry over Fiji Islands was shot from on-ground in a CNN video [1] Figure 3, which partially captured the break-up sequence.

Figure 1 MIR (Original image: NASA/Crew of STS-91 http://spaceflight.nasa.gov/gallery/images/shuttle/sts-91/html/91727051.html).

A further analyses of the CNN video was performed [2] and many information regarding the MIR re-entry were extrapolated. These information include the (plausbile) identification of the main parts visible in the video using ballistic coefficient estimtion, altitude and velocities of the components during the observed break-up sequnce and possible range of altitude for the MIR modules mechanical separation. Table 1 summarizes some of these information, relevant for this analysis. Figure **Error! Reference source not found.** shows the extrapolated location of the aerothermal break-up of the MIR lead object and debris footprint.

MIR
• Mechanical break-up of the station modules is visible at 77km, • Thermal fragmentation becomes the break-up driver at 70 km. • The large thermal mass delayed the break-up in general

Table 1 MIR - Derived break-up phenomenology [2].

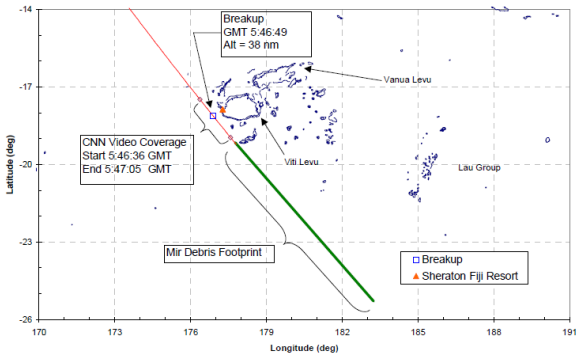

Figure 2 MIR - STERN report on re-entry analyses [2].

Figure 3 MIR - CNN video at 6.9 seconds.

2.2 SKYLAB Space station

Figure 4 SKYLAB (Source: NASA /Crew of Skylab 4. - http://grin.hq.nasa.gov/ABSTRACTS/GPN-2000-001055.html).

The USA Space Station SKYLAB was launched by NASA on May 14 1973 and performed a partially controlled re-entry on July 11 1979, targeting the safe area of the south Indian Ocean. However, the space station had no capability of further propulsive manoeuvre during its re-entry and an under-predicted drag modulation results in the partially overshot of the target area [3]. As consequence, on-ground debris were found on South Western Australia [4], as shown in Figure 4.

SKYLAB
• The Orbital Work Station (OWS) Solar Array system broke off at 114km, • The Apollo Telescope Mount (ATM) Solar Array System broke off at 96 km, • The ATM / OWS mechanically separated at 78km.

Table 2 SKYLAB - derived break-up phenomenology [4]

Among the recovered debris, one belonged to the ATM module (ATM-CMG), five were on the OW module (OW-H_2O Tank, OW-Vault, OW-Heat exchanger, OW freezer and OW- TACS) and one was on the AS module (AS-O_2bottle) Table 2 summarizes the relevant information extrapolated for this test case:

2.3 DELTA II – second stage

Delta II was a launch vehicle of the Delta rocket family which started service in 1989. On January 22, 1997 a Delta II Second Stage re-entered over Canada and the United States, and several fragments were found on ground. Figure 6 shows the lightweight fragment landed near Turley, the cylindrical propellant tank, the thrust chamber that landed near Seguil and the Spherical gas tank. An analysis of this re-entry and of the re-entry of a Delta II third stage occurred in 2001, are available in [7]. **Error! Reference source not found.** summarized the extrapolated break-up phenomenology.

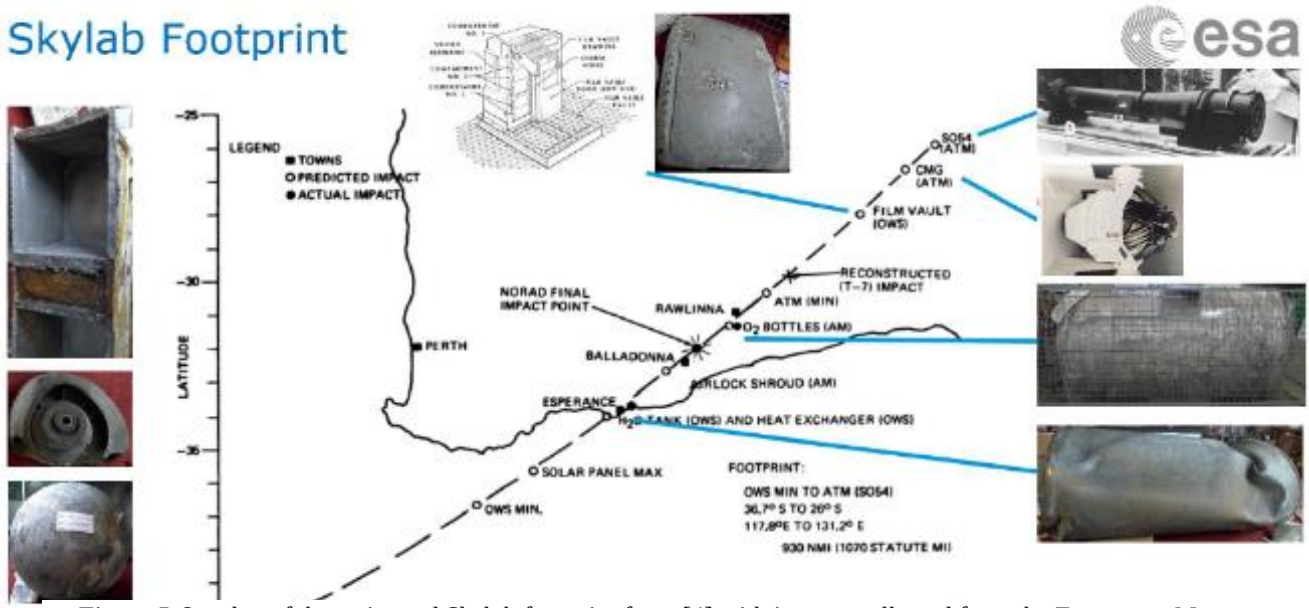

Figure 5 Overlay of the estimated Skylab footprint from [4] with images collected from the Esperance Museum contained fragments mentioned [ESA] [5].

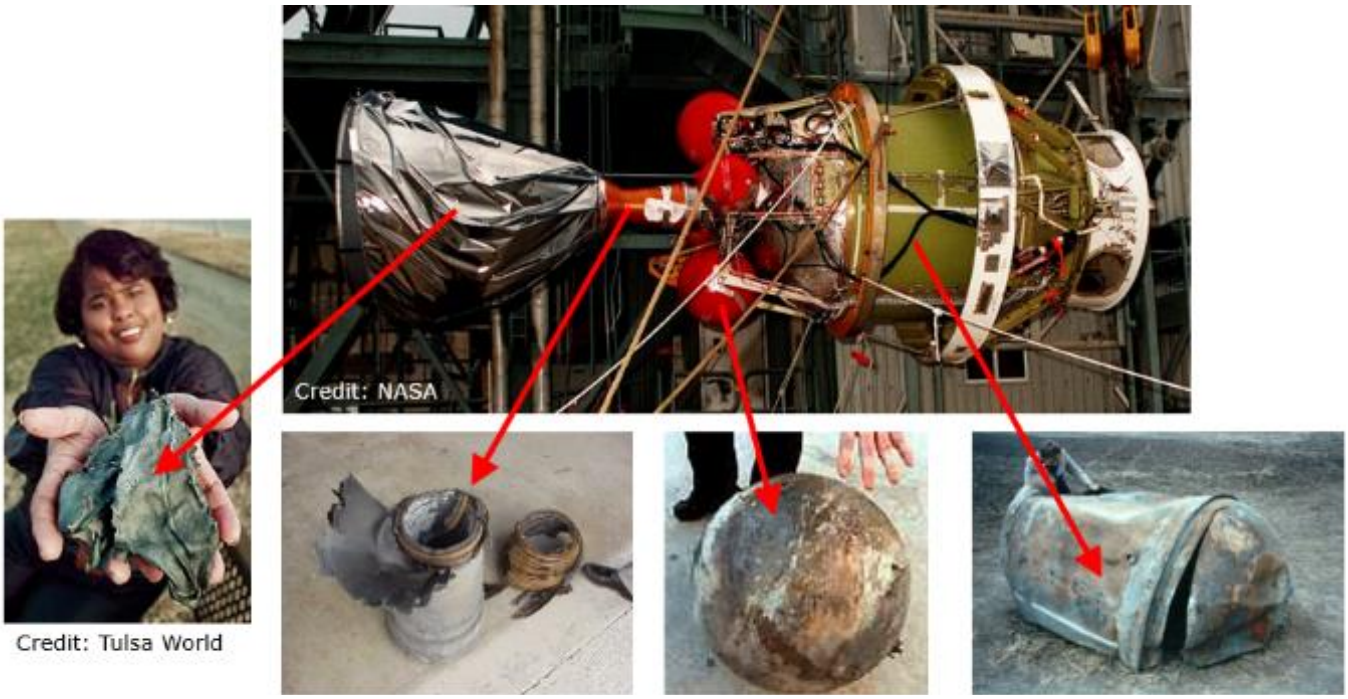

Figure 6 Debris from Delta II Second Stage re-entry[7].

Delta II – Second stage
• Major break-up at 78.8538 km, • Maximum temperature during re-entry between 1000 and 1300 ºC.

Table 3 Delta II - Second Stage - Derived break-up phenomenology [7].

3 METHODOLOGY.

3.1 Genetic Algorithm approach

The proposed work employs a genetic algorithm approach to retrieve the most statistically probable break-up conditions for large vehicles. Genetic algorithms are probabilistic approach based on the Darwinian principle of natural selection, used to solve optimization and search problems. In few words, a genetic algorithm starts with one provided individual (first solution guess), which genes need to be optimized. In the framework of this work, each individual is a set of plausible break-up altitudes for a selected number of connections of the re-entry object, with each gene representing the break-up altitude for one of these selected connections. In this work, the initially guessed solution, regardless to the specific test case, was a set of break-up altitude (genes) all equal to the conventionally accepted break-up altitude of 78 km [9]. As a first step, this individual is altered in order to create a population of similar individuals, i.e. the initial population. In this work, this alteration is performed by sampling a Gaussian distribution around the initial guesses, with a standard deviation of 3 km. The size of the initial population is an input parameter of the genetic algorithm, that was chosen to be equal to 30 individuals. This initial population is then evaluated using ad-hoc evaluation function in order to assign a set of fitnesses to each individual. The fitnesses represent the values that need to be minimize (minimal optimization) by the genetic algorithm. In this work, the fitnesses are the mean square error between the observed and the simulated data (impact points for SKYLAB and Delta II-Second Stage and break-up conditions for the MIR test case). Analogous to natural selection, the worst individuals of the population, according with their fitnesses, are discharged (extinguished), while the others undergo the mating step which selects the individuals for the mating pool, i.e. the parents. Individuals with the lowest fitnesses can be selected more than once for the mating pool. For each individual of the mating pool, two user-defined coefficients (cxpd, mutpb) provide the probabilities to have their genes mutated or crossed with other individuals. As result of all these steps, a new population is created (children). The iterative process continues until the number of iterations is equal to the user-defined number of generations for the evolution process, that for this analysis was set equal to 500. The best individuals across the whole evolution process are stored in ascend order w.r.t. their fitnesses in the Hall of Fame (HOF). At the end of the analysis, the first individuals of the HOF represent the best solutions, i.e. the set of break-up altitudes which match the observed data at best.

3.2 Implementation

The python package DEAP [15] was used for the implementation of the evolutionary algorithms, while the ESA-DRAMA3.0.4/SARA software [12], [13], [14] was used for the object modelling and the re-entry simulations. The features of the SARA break-up software includes the possibility to define break-up triggers for model connections and for the released of nested components, so that each set of break-up conditions (individual) generated by the genetic algorithm process was provided as break-up trigger for the leading components of the model. The results from the re-entry simulation were compared with the available observation for the specific test case, in order to evaluate the fitnesses for the individual.

A preliminary phase of parameter tuning, showed the best results for the eaMuPlusLambda algorithm [16], with cxpb and mutpb indexes equal to 0.3 and 0.5 respectively. Figure 7 shows a simplified scheme of the genetic algorithm approach implemented for this study.

The simplified models for the MIR, SKYLAB and Delta II Second Stage used for this study, shown in Figure 8, Figure 9 and Figure 10, have 62, 23 and 15 number of primitives respectively.

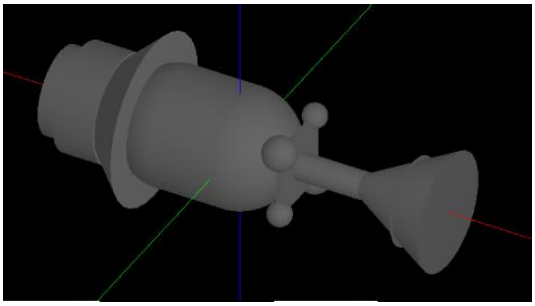

Figure 8 Delta II - Second Stage ESA-DRAMA model.

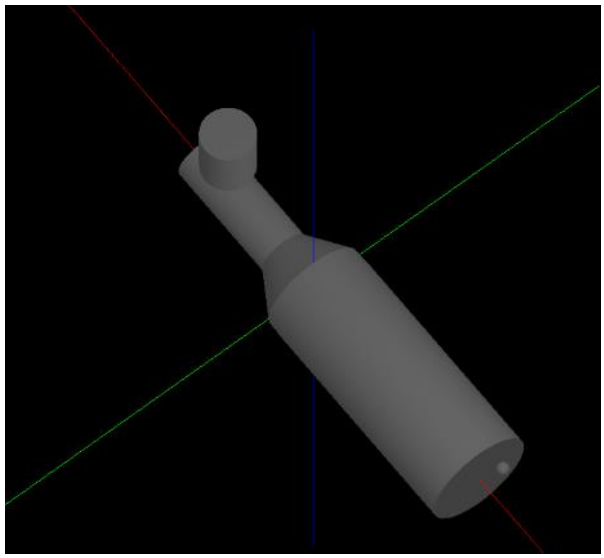

Figure 9 SKYLAB - ESA-DRAMA model.

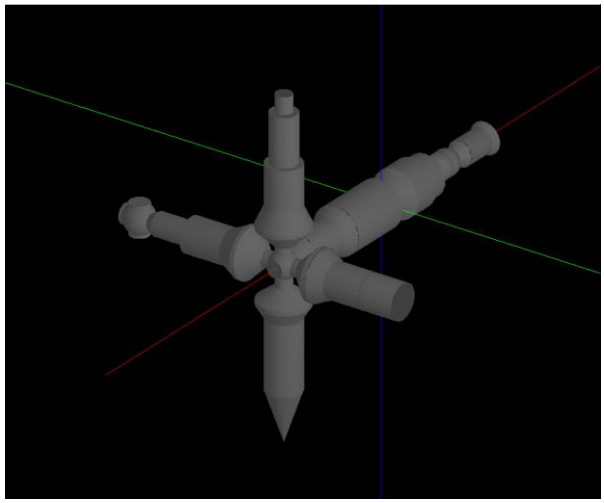

Figure 10 MIR-ESA-DRAMA model.

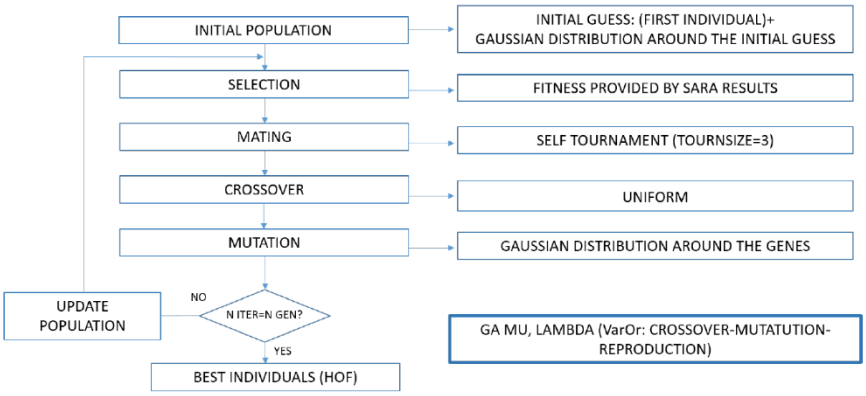

Figure 7 Genetic Algorithm scheme.

4 RESULTS.

4.1 MIR.

In agreement with [2], the following nomenclature is used for the MIR major components:

Object	MIR component
A	MIR Core Module,
B	Kvant1 Module
C	Progress Cargo Supply Craft
D	Krystall, Space Shuttle
E	Piroda Module
F	Spektr Module
I	Kvant2
A-1	Separates from A (7.3 sec into CNN video)
C-1	Separates from C (11.9 sec into CNN video)
D-1	Separates from D (2 sec into CNN video)

Table 4 MIR modules nomenclature.

A major aerothermal break-up and a minor break-up (A-1 separates from A) for the leading object A were observed in (or postulated based on) the CNN video, at 13 and 7.3 seconds respectively. The separation of the object C1 from C and D1 form D were also observed at 11.9 and 2 seconds into the CNN video respectively. The mechanical break-up of the major objects C through I, occurred before the beginning of the CNN video, while separation between B and C is visible at 3 sec into the CNN video, but no information regarding this last break-up was extrapolated due to intermittent coverage.

Separation	Range of value [m]	Initial guess [m]
A from B+C	[71116.8 - 120000]	78000
B from C	[69913 - 75000]	70000
A from D	[71116.8 - 120000]	78000
A from E	[71116.8 - 120000]	78000
A from F	[71116.8 - 120000]	78000
A from I	[71116.8 - 120000]	78000

Table 5 MIR - Break-up altitudes to be optimized (individuals).

Furthermore, the separation between A and B+C is assumed to happen one second prior to the start of the video, based upon the observed separation rate.

Based on these information, the break-up altitudes (individual) that need to be optimized through the genetic algorithm for the MIR test case were identified, as summarized in Table 5. The lower limit for the range of values for the break-up altitudes, in this case, is equal to the highest observed break-up, since the hypothesis is that the break-ups in Table 5 occurred prior the CNN video. The only exception is made for the B/C objects separation, which range of values is approximatively matching the CNN video altitudes coverage. Finally, the true anomaly (and therefore re-entry epoch) is added to the individual as a parameter to be optimized, in order to find the best fitting re-entry condition along the given MIR orbit [3]. This is a rough approximation, since the other orbital parameters are kept fixed, even though the eccentricity and semimajor axis are expected to variate approaching the dense atmosphere.

The rest of the available information was used for the evaluation of the individuals. More in details, for each of the known break-up altitudes in Table 6 (check points), the break-up time and velocity from the simulation results were compared with the information provided in [2]. Furthermore, since there is no direct connection between the starting time of the CNN video and the starting time of the simulation, considering that the true anomaly and re-entry epoch are fitting parameters, the information regarding the break-up times were used in relative sense, i.e. the time difference between two consecutive break-up was used instead of the absolute break-up time, Table 7, in order to compare the break-up temporal sequence regardless the starting time of the simulation.

As a further criteria, the latitude and longitude at the simulated break-up conditions, for each of the check points, were compared to the break-up latitude and longitude that were estimated combining the MIR footprint, the coordinates of the MIR major mechanical separation and the in-track separation of the observed objects [2]. This is a rough approximation, considering the lack of information in terms of cross-track separations, but it is implicitly justified by simplified models and the nature of the current work that does not aim to provide precise solutions, rather a statistically meaningful range of values.

Separation	time into CNN video[sec] [2]	Break-up altitude [m][2]	v [m/sec] [2]	Estimated lat [deg]	Estimated lon [deg]
A-1 from A	7.3	70598.24	7247.8	-18.3	177.2
A-2 from A	13	69913.0	7221.3	-18.8	177.5
C-1 from C	11.9	70079.68	7226.2	-18.6	177.4
D-1 from D	2	71116.8	7270.4	-18.0	177.0

Table 6 MIR - Check points information for individual's evaluation.

Temporal constrains
Time between D-1/D separation and A-1/A separation = 5.3 sec
Time between A-1/A separation and C-1/C separation = 6.6 sec
Time between C-1/C separation and A-2/A separation = 1.1 sec

Table 7 MIR - Additional constrains for the individual evaluation.

Considering the different order of magnitude of the reference values in Table 6 and Table 7, the differences between reference values and simulated values (fitnesses) were expressed in terms of percentage w.r.t. the reference values themselves, in order to balance the relevance of each fitness value for the optimization process.

The 50 best individuals of the HOF obtained as results of the above presented methodology provided statistical insights of the altitude range at which each separation occurred, as shown in Table 9.

Parameter	Reference [2]	Best individual
Epoch	2001-03-22 05:48:31.00	2001-03-22 05:31:31.00
sma [km]	6524.3	6524.
ecc [-]	0.009664	0.009664
inc [deg]	51.6	51.6
raan [deg]	256.0	256.0
aop [deg]	239.7	239.7
tan [deg]	240.0	170.41

Table 8 MIR re-entry conditions.

Separation	Best Individual break-up altitude[m]	Range of values for break-up altitude[m]	Average value[m]
A from B+C	86652.566	93789.498 73306.459	82702.663
B from C	70198.103	74716.67 69936.028	73227.28
A from D	76556.319	88966.182 72611.024	79898.267
A from E	77594.7989	87732.974 71696.984	76792.971
A from F	78196.306	97465.810 71835.198	78835.291
A from I	76804.901	89214.915 71906.164	80281.811

Table 9 MIR- Best individuals and range of values for the best 50 individuals of the HOF.

The re-entry conditions used as reference, alongside with the re-entry initial conditions for the best performing simulation, are shown in Table 8, while the ESA-DRAMA/SARA results for the best performing solution are shown in Figure 11.

Finally, the fitnesses for the best solution are summarized in Table 10. For the temporal constrains introduced in Table 7, the best individual solution obtained a difference w.r.t. the targeted vales or -1.84 sec, -2.75 sec and -2.6 sec respectively.

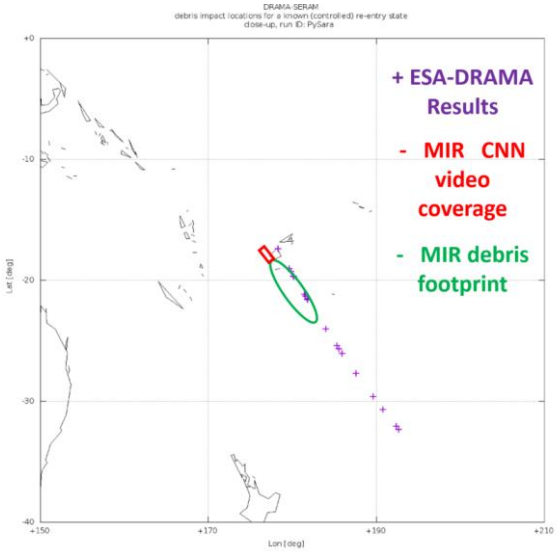

Figure 11 MIR – Video coverage with estimated debris footprint [2] and best individual re-entry results.

4.2 SKYLAB.

For the SKYLAB test case, the available information were the footprint of the survived debris [3][4][5]. Therefore, the break-up altitude of the connections between the main structure and the objects retrieved on-ground were defined as the individual for the genetic algorithm, as summarized in Table 13. The individual evaluation, in this case, was performed comparing the debris impact locations obtained from the simulated re-entry against the documented impact locations summarized in Table 11.

Separation	Velocity [m/sec] [2]	Best individual Velocity [m/sec]	Estimated lat [deg]	Best Individual lat[deg]	Estimated lon[deg]	Best individual lon[deg]
A-1 from A	7247.8	7230.0	-18.3	-18.058	177.2	178.804
A-2 from A	7221.3	7196.0	-18.8	-18.326	177.5	179.025
C-1 from C	7226.2	7258.0	-18.6	-18.202	177.4	178.923
D-1 from D	7270.4	7354.0	-18.0	-18.0	177.0	178.757

Table 10 MIR - Best individual's fitnesses.

Furthermore, as for the MIR test case, the true anomaly at the re-entry condition for the simulation was added to the individual as parameter to be optimized.

Debris [3][4][5]	Impact lat [°]	Impact lon [°]
ATM-CMG	-26.7	130.3
OW-H_2O Tank	-33.8	122.05
OW-Vault	-28.0	129.0
AS-O_2Bottle	-31.15	125.3
OW-Heat Exchanger	-33.75	122.1
OW-Frezeer	-33.822	122.106
OW-TACS-GN2-T-01	-33.256	122.589

Table 11 SKYLAB - Check points information for individual's evaluation (Survived debris impact locations [3] [4] [5]).

Separation/Release	Proposed range of values [m]	Initial guess [m]
OW-N_2Tank separation	60000 - 120000	78000
ATM nested components release (CMG)	60000 - 120000	78000
OW nested components release (H_2O Tank, freezer, vault, TACS)	60000 - 120000	78000
AS nested components release (O_2 bottle)	60000 - 120000	78000

Table 13 SKYLAB Break-up altitudes to be optimized (individuals).

With the inputs presented in the previous Table 13 and Table 11, the results of the best 50 individuals of the HOF provided the range of values shown in Table 12, alongside with the best individual break-up altitudes. The fitnesses of this best individual are summarized in Table 14, while its re-entry condition are shown in Table 15. Finally, Figure 12 shows the re-entry simulation results for the best individual for the SKYLAB test case.

Separation	Best Individual break-up altitude[m]	Range of values for break-up altitude[m]	Average value[m]
OW-N_2Tank separation	68748.280	83716.762 70872.858	76313.484
ATM nested components release	81985.386	83926.593 60028.934	77642.737
OW nested components release	63043.230	85292.217 76415.199	66487.919
AS nested components release	77223.709	79728.462 71819.223	81136.914

Table 12 SKYLAB- Best individuals and range of values for the best 50 individuals of the HOF.

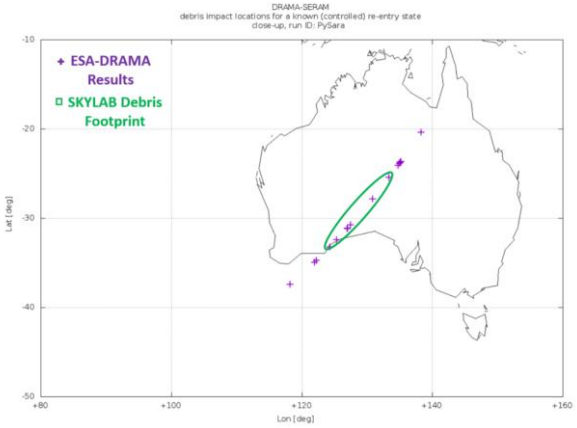

Figure 12 SKYLAB Debris footprint [4] and re-entry results for the best individual.

Separation	Impact lat [deg]	Best Individual lat[deg]	Impact lon[deg]	Best individual lon[deg]
ATM-CMG	-26.7	-26.7	130.3	132.058
OW-H_2O Tank	-33.8	-30.576	122.05	127.665
OW-Vault	-28.0	-27.895	129.0	130.759
AS-O_2Bottle	-31.15	-32.244	125.3	125.59
OW-Heat Exchanger	-33.75	-30.927	122.1	127.239
OW-Frezeer	-33.822	-32.905	122.106	124.733
OW-TACS-GN_2-T-01	-33.256	-32.99	122.589	124.62

Table 14 SKYLAB Best individual's fitnesses.

Parameter	Reference [3]	Best individual
Epoch	1979-07-11 15:20:22.318	1979-07-11 15:22:26.318
sma [km]	6477.7573	6477.7573
ecc [-]	9.532353E-4	9.532353E-4
inc [deg]	50.026997	50.026997
raan [deg]	325.56937	325.56937
aop [deg]	23.599459	23.599459
tan [deg]	136.64655	146.682

Table 15 SKYLAB - Re-entry conditions.

4.3 Delta II – Second Stage

For the last test cases analysed in this work, as for the SKYLAB test case, the available data was the footprint of the survived fragments [7]. Similar to what was done for the SKYLAB the case, the break-up altitudes of the connections among the main structure and the objects retrieve on-ground were selected as individuals for the optimization. These individuals are shown in Table 16. Also for this last test case, the true anomaly is optimized by the genetic algorithm, as for the break-up altitudes.

Separation/Release	Proposed range of values [m]	Initial guess [m]
Propellant tank-engine support	60000 - 120000	78000
Gas tank-engine support	60000 - 120000	78000
Fragment-Nozzle	60000 - 120000	78000
Thrust Chamber-Support	60000 - 120000	78000
Thrust Chamber-Nozzle	60000 - 120000	78000

Table 16 Delta II Second Stage- Break-up altitudes to be optimized (individuals).

Separation	Best Individual break-up altitude[m]	Range of values for break-up altitude[m]	Average value[m]
Propellant tank-engine support	74925.568	78193.015 66581.97	73868.833
Gas tank-engine support	86398.93	93043.446 81287.994	86023.845
Fragment-Nozzle	75358.82	76650.144 72387.823	74521.734
Thrust Chamber-Support	76450.30	86324.024 68076.041	77060.154
Thrust Chamber-Nozzle	66612.30	82453.513 61990.553	69240.617

Table 17 Delta II Second Stage- Best individuals and range of values for the best 50 individuals of the HOF.

The most plausible range of values for the altitude break-up of the main components of the Delta II – Second Stage, according with the best 50 individuals form the HOF are summarized in Table 17, alongside with the best individual solution. This best individual is obtained with the initial conditions showed in Table 18. The fitnesses and re-entry simulation results for this best individual are shown in Figure 13and Table 19 respectively.

Parameter	Reference [7]	Best individual
Epoch	1997-01-22 09:02:32.420	1997-01-22 09:03:11.420
sma [km]	6495.1826	6495.1826
ecc [-]	0.002244016	0.002244016
inc [deg]	96.57158	96.57158
raan [deg]	344.69855	344.69855
aop [deg]	98.30452	98.30452
tan [deg]	262.00864	273.760

Table 18 Delta II Second Stage Re-entry parameters.

Separation	Impact lat [deg]	Best Individual lat[deg]	Impact lon[deg]	Best individual lon[deg]
Propellant Tank	30.644	-97.622	30.647 -	-97.084
Sphere (gas tank)	29.712	-97.879	29.462	-97.339
Fragment	36.249	-95.956	36.273	-95.812
Thrust Chamber	29.576	-97.92	29.049	-97.426

Table 19 Delta II Second Stage Best individual's fitnesses.

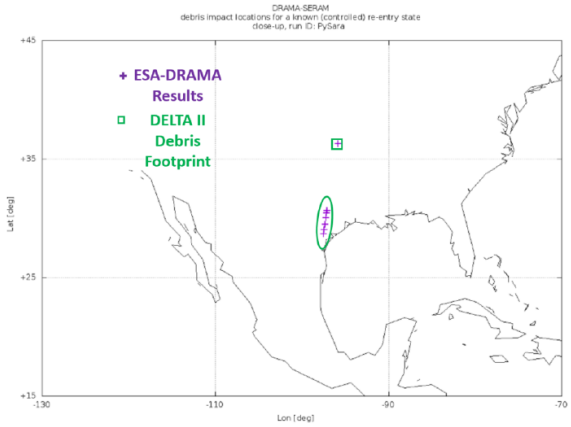

Figure 13 Delta II Second Stage – Debris footprint [7] and re-entry results for the best individual.

4.4 Overall Results

With the purpose to extrapolate an overall range of values for re-entry conditions for large objects, the altitude of the break-up connections and the velocity at break-up condition for the selected components of the re-entering object for the best 50 individuals, were collected for the three analysed test cases. The results obtained are summarized in the following Figures.

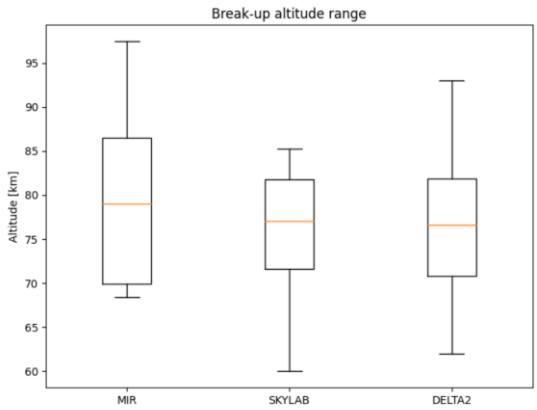

Figure 14 Range of values for the break-up altitude for the fitted components of the three analysed test cases.

In Figure 14, the range of values for the break-up altitudes for the MIR test case has a lower limitation imposed by the minimum break-up altitude observed in the CNN video.

As visible, the average values is consistent among the three cases, placing the average main break-up between 77-78 km. This result is consistent with the break-up phenomenology summarized in Table 1, Table 2 and Table 3. The overall range of averaged break-up altitude, for all the objects components analyses is 66.487 – 86.023 km.

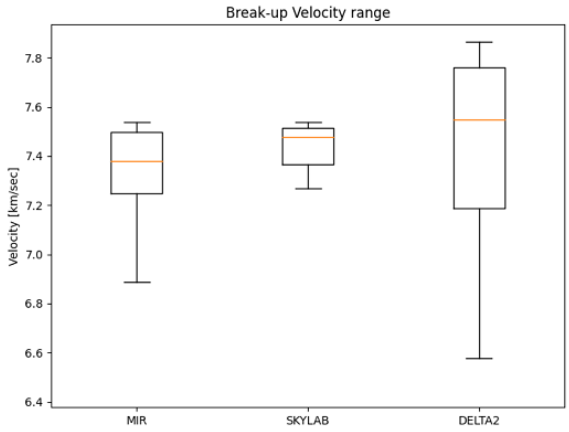

Figure 15 Range of values for the break-up velocity for the fitted components of the three analysed test cases.

Figure 15 shows a quite similar overall range for the velocity at the break-up condition for the three tested cases, with values between 6.6 and 7.8 km/sec.

5 CONCLUSIONS.

Foreseeing the disposal of the ISS, in this work, a genetic algorithm approach was applied with the aim to recover a possible range of values for the break-up altitude for the re-entries of large objects on the base of observed break-up sequences or debris footprint. The proposed methodology uses simplified geometries in order to enable the possibility to perform a large number of simulations and extract statistically significant results rather than precise solutions. Three test cases were analysed, the Russian space station MIR, re-entered on 2001, the USA space station SKYLAB, re-entered in 1979 and the Delta II Second Stage, which re-entered in 1997.

Starting from the observations, a possible scenario for the break-up sequences for these three events were obtained. More relevant, a range of possible values for break-up altitudes based on the best 50 solutions of the genetic algorithm was identified. This overall range of values is estimated between 66.487 – 86.023 km., with an average values between 77 and 78 km, which appears to be consistent with break-up phenomenology extracted from the observations and available in literature.

Finally, range of values was also obtained for velocity at the break-up condition, with values spanning between 6.6 and 7.8 km/sec.

6 REFERENCES.

1. http://www.cnn.com/2001/TECH/space/03/23/williams.debrief/indes.ht
2. R. G. Stern (2003). Analysis of Mir Reentry Breakup. AEROSPACE REPORT NO. TR-2003(8506)-1.
3. NASA's Systems Analysis and Integration Laboratory (1980). SKYLAB REACTIVATION MISSION REPORT. NASA TM-78267
4. P. E. Dreher, R. P. Little, and G. Wittenstein (1981). Skylab Orbital Lifetime Prediction and Decay Analysis. NASA Technical Memorandum 78308.
5. S. Lemmens (2019). On the Re-Entry of Large Artificial Space Objects and Resulting Footprint Estimation. Proceeding at the 10th IAASS Conference.

6. Stern, R. G. (2008). Reentry Breakup and Survivability Characteristics of the Vehicle Atmospheric Survivability Project (VASP) Vehicles. AEROSPACE REPORT NO. TR-2008(8506)-3.

7. W. Ailor, W. Hallman, G. Steckel, M. Weaver (2005), Analyses if reentered debris and implications for survavibility modelling, Proceedings of the 4th ESD Conference, Darmstadt, Germany.

8. European Space Agency (2017). ESA Re-entry Safety Requirements. ESSB-ST-U-004.

9. H. Klinkrad, B. Fritsche, and T. Lips (2004). A Standardized Method for Re-Entry Risk Evaluation, Proceedings of the 55th International Astronautical Congress, Vancouver, Canada.

10. D. Leiser, et al, (2018). Determining Reentry Breakup Forces in an Impulse Facility. Proceedings of 4th Internation Space Debris Re-entry Workshop, Darmstadt, Germany .

11. F. Zander, et al, (2017). Numerical Flow Analysis of The ISS Re-entry. Proceedings of 7th European Conference on Space Debris, Darmstadt, Germany.

12. R. Kanzler, et al, (2017). Upgrade of DRAMA's Spacecraft Entry Survival Analysis Codes. Proceedings of 7th European Conference on Space Debris, Darmstadt, Germany.

13. European Space Agency (2019), Space Debris User Portal, https://sdup.esoc.esa.int/

14. S. Sanvido (2019). PyDrama. ESA-ECSL Sppace Debris Regulation, Standard and Tool Workshop.

15. F.A. Fortin, F.M, De Rainville, M.A. Gardner, et. al. (2012), DEAP: Evolutionary algorithms made easy, Journal of Machine Learning Research 13:2171-2175.

16. https://deap.readthedocs.io/en/master/api/algo.html

17. European Space Agency (2019), DIVE - Guidelines for Analysing and Testing the Demise of Man Made Space Objects During Re-entry, ESA-TECSYE-TN-018311.

18. Bastida Virgili, B., Krag, H., Lips, T., et. al., (2010) Simulation of the ATV Re-entry Observations, Proceedings of the 4th IAASS Conference, ESA, Hunsville, United State.

19. Lemmens, S., Bastida Virgili, B., Funke, Q., et. al.(2016), From end-of-life to impact on ground: An overview of ESA's tools and techniques to predicted re-entries from the operational orbit down to the Earth's surface, Proceedings of the 6th ICATT Conference, Darmstad, Germany, 2016.

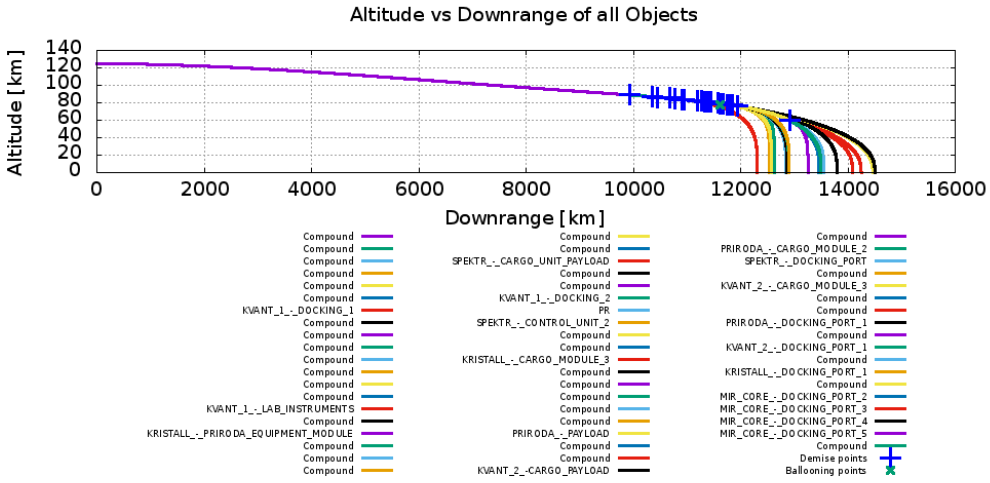

Figure 16 MIR - Best individual ESA-DRAMA/SARA re-entry results - Downrange.

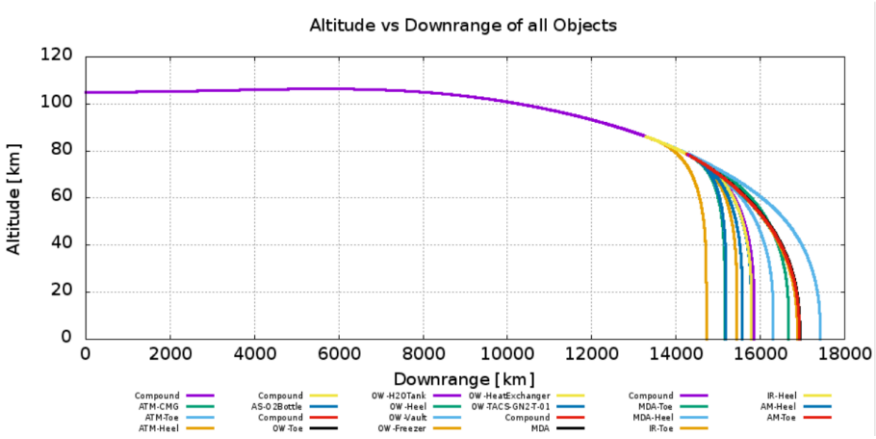

Figure 17 SKYLAB Best individual ESA-DRAMA/SARA re-entry results - Downrange.

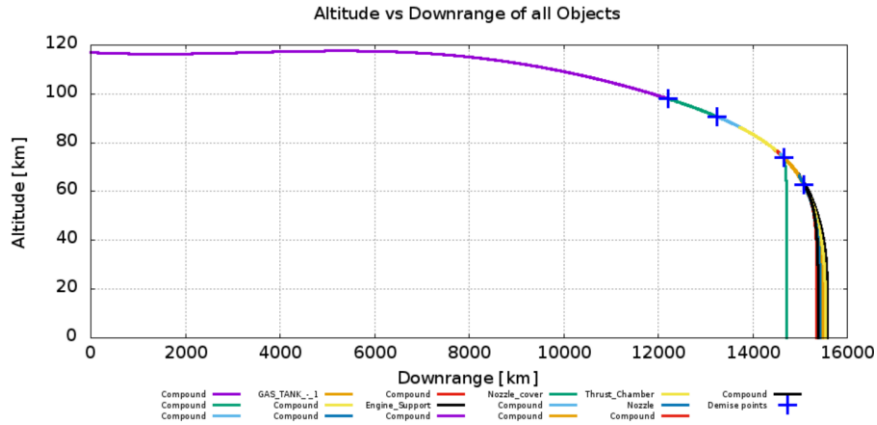

Figure 18 Delta II Second Stage - Best individual ESA-DRAMA/SARA re-entry results - Downrange.